Search for the pentaquark via the $P^0_{\bar{c}s} \to K^{*0}K^-p$ decay

Fermilab E791 Collaboration

E. M. Aitala,[i] S. Amato,[a] J. C. Anjos,[a] J. A. Appel,[e] D. Ashery,[n] S. Banerjee,[e] I. Bediaga,[a] G. Blaylock,[h] S. B. Bracker,[o] P. R. Burchat,[m] R. A. Burnstein,[f] T. Carter,[e] H. S. Carvalho,[a] N. K. Copty,[l] L. M. Cremaldi,[i] C. Darling,[r] K. Denisenko,[e] A. Fernandez,[k] G. F. Fox,[l] P. Gagnon,[b] S. Gerzon,[n] C. Gobel,[a] K. Gounder,[i] A. M. Halling,[e] G. Herrera,[d] G. Hurvits,[n] C. James,[e] P. A. Kasper,[f] S. Kwan,[e] D. C. Langs,[l] J. Leslie,[b] J. Lichtenstadt,[n] B. Lundberg,[e] S. MayTal-Beck,[n] B. T. Meadows,[c] J. R. T. de Mello Neto,[a] D. Mihalcea,[g] R. H. Milburn,[p] J. M. de Miranda,[a] A. Napier,[p] A. Nguyen,[g] A. B. d'Oliveira,[l] K. O'Shaughnessy,[b] K. C. Peng,[f] L. P. Perera,[c] M. V. Purohit,[l] B. Quinn,[i] S. Radeztsky,[q] A. Rafatian,[i] N. W. Reay,[g] J. J. Reidy,[i] A. C. dos Reis,[a] H. A. Rubin,[f] D. A. Sanders,[i] A. K. S. Santha,[c] A. F. S. Santoro,[a] A. J. Schwartz,[c] M. Sheaff,[d,q] R. A. Sidwell,[g] A. J. Slaughter,[r] M. D. Sokoloff,[c] J. Solano,[a] N. R. Stanton,[g] R. J. Stefanski,[e] K. Stenson,[q] D. J. Summers,[i] S. Takach,[r] K. Thorne,[e] A. K. Tripathi,[g] S. Watanabe,[q] R. Weiss-Babai,[n] J. Wiener,[j] N. Witchey,[g] E. Wolin,[r] S. M. Yang,[g] D. Yi,[i] S. Yoshida,[g] R. Zaliznyak,[m] C. Zhang[g]

[a] *Centro Brasileiro de Pesquisas Físicas, Rio de Janeiro, Brazil*

[b] *University of California, Santa Cruz, California 95064*

[c] *University of Cincinnati, Cincinnati, Ohio 45221*

[d] *CINVESTAV, 07000 Mexico City, DF Mexico*

[e] *Fermilab, Batavia, Illinois 60510*

[f] *Illinois Institute of Technology, Chicago, Illinois 60616*

[g] *Kansas State University, Manhattan, Kansas 66506*

[h] *University of Massachusetts, Amherst, Massachusetts 01003*

Preprint submitted to Elsevier Preprint *17 December 1998*

[i] *University of Mississippi, University, Mississippi 38677*
[j] *Princeton University, Princeton, New Jersey 08544*
[k] *Universidad Autonoma de Puebla, Mexico*
[l] *University of South Carolina, Columbia, South Carolina 29208*
[m] *Stanford University, Stanford, California 94305*
[n] *Tel Aviv University, Tel Aviv, 69978 Israel*
[o] *Box 1290, Enderby, British Columbia, V0E 1V0, Canada*
[p] *Tufts University, Medford, Massachusetts 02155*
[q] *University of Wisconsin, Madison, Wisconsin 53706*
[r] *Yale University, New Haven, Connecticut 06511*

We have searched for evidence of the production and decay of a neutral bound-state pentaquark, one of a predicted doublet of states: $P^0_{\bar{c}s} = |\bar{c}suud\rangle$ and $P^-_{\bar{c}s} = |\bar{c}sddu\rangle$. Specifically, we have searched for the decay $P^0_{\bar{c}s} \to K^{*0}K^-p$ in data from Fermilab experiment E791, in which a 500 GeV/c π^- beam interacted with nuclear targets. We find mass-dependent upper limits at the 90% confidence level for the ratio of cross section times branching fraction of this decay relative to that for the decay $D_s^- \to K^{*0}K^-$. The upper limits vary between 0.016 and 0.036 for $M(P^0_{\bar{c}s})$ between 2.75 and 2.91 GeV/c^2, assuming a pentaquark lifetime of 0.4 ps.

The spectrum of observed hadrons generally fits into multiplets of two- and three-quark states. The mass differences within these multiplets can be explained by effective quark masses and the color-hyperfine (CH) interaction in the QCD Hamiltonian. Calculations done using the CH interaction predict the existence of particles consisting of more than three quarks. Jaffe [1] predicted the existence of the H dibaryon, $H = |uuddss\rangle$, and extensive efforts have been made to find it experimentally [2]. Lipkin [3] and Gignoux *et al.* [4] have proposed that a doublet of states, the $P^0_{\bar{c}s} = |\bar{c}suud\rangle$ and the $P^-_{\bar{c}s} = |\bar{c}sddu\rangle$ and their charge conjugate states, may exist and be stable against strong decays. These are referred to as pentaquarks.

There is a threshold for the strong decay of each of the pentaquarks. Above 2.907 GeV/c^2, the $P^0_{\bar{c}s}$ can decay to D_s^- and a proton. Calculations done using only the CH interaction predict pentaquark masses which vary from 150 MeV/c^2 below the D_s^-–nucleon threshold to a few tens of MeV/c^2 below threshold, depending on how SU(3)$_{flavor}$ symmetry is broken and how the mass of the charm antiquark is taken into account [4]. Contributions to the binding energy from other components of the Hamiltonian are also model dependent. Calculations done using an instanton model [5], bag models [6,7], and a Skyrme model [8] conclude that, depending upon the choice of parameters, the pentaquark is bound or is a near-threshold resonance. If bound, the lifetime is expected to be similar to that of charm particles, with the exact value depending upon unknown internal structure. In a description of the pentaquark as an off-shell charm meson and a spectator baryon, it is assumed that the off-shell meson decays to the same decay products as the free meson. The pentaquark lifetime would then be similar to that of the D_s^- charm meson, 0.47 ps[9]. A description of the pentaquark as a five-quark state allows more interactions among the quarks and consequently may lead to a shorter lifetime. In the work described here, we have considered lifetimes ranging from 0.1 ps to 1.0 ps, and $P^0_{\bar{c}s}$ masses ranging from 2.750 GeV/c^2 (the lowest predicted) to the threshold at 2.907 GeV/c^2.

Various mechanisms for pentaquark production have been discussed by Lipkin [10]. However, only crude estimates of the pentaquark production cross section exist in the literature. One mechanism considers the production of all five quarks in the interaction [11] and is based on an empirically motivated equation which predicts reasonably well the production cross section of other charm particles. Another mechanism is the coalescence model, in which pentaquark components such as the D_s^- and a nucleon are produced in the reaction and fuse into one particle while in overlapping regions of phase-space[12]. In both models, pentaquark production is primarily central; i.e., the spectrum of the scaled longitudinal momentum (x_F) peaks near zero. Estimated pentaquark production cross sections range between 10^{-4} and 10^{-2} times that of the D_s^-[11,12].

In this letter we report results from a search for pentaquark production and decay via $P^0_{\bar{c}s} \to K^{*0}K^-p$. We have previously reported the results of a search for $P^0_{\bar{c}s} \to \phi\pi^-p$[13] which contains the same stable hadrons in the final state ($K^-K^+\pi^-p$). We measure the product of cross section times branching-fraction ($\sigma \cdot \mathrm{B}$) for $P^0_{\bar{c}s} \to K^{*0}K^-p$ relative to that for $D_s^- \to K^{*0}K^-$. This ratio is the quantity measured most directly, and it is the quantity predicted most easily by theory. For each of these decay modes we consider the sum of particle and antiparticle, and charge conjugate modes are implied throughout this paper.

We use data from experiment E791[14] which recorded 2×10^{10} 500 GeV/c π^--nucleon interactions during the 1991/92 fixed-target run at Fermilab. The segmented target consisted of one platinum foil and four diamond foils separated by gaps of 1.34 to 1.39 cm. Each foil was approximately 0.4% of an interaction length thick (0.5 mm for platinum and 1.6 mm for diamond). Pentaquarks with lifetimes in the range expected and produced with momenta in the range for which the detector has good geometric acceptance should decay most frequently in the air gaps between the foils. As for other charm signals, the backgrounds for pentaquark signals should be lower in these gaps. For comparison, the average decay length of a D_s of momentum 80 GeV/c, roughly the mean value we observe, is approximately 6 mm. There were six planes of silicon microstrip detectors (SMDs) and eight proportional wire chambers (PWCs) used to track the beam particles. The downstream detector consisted of 17 planes of SMDs for vertex detection, 35 drift chamber planes, two PWCs, and two magnets for momentum analysis. Two multicell threshold Čerenkov counters[15] with nominal pion thresholds of 6 GeV/c and 11 GeV/c provided charged π, K, and p identification. Electromagnetic and hadronic calorimeters were used for online triggering and for electron identification. Two planes of scintillators behind an equivalent of 2.4 m of iron provided muon identification. An interaction pre-trigger required a beam particle and an interaction in the target. A very loose transverse energy trigger based on the energy deposited in the calorimeters and a fast data acquisition system [16] allowed us to collect data at a rate of up to 30 Mbytes/s with 50μs/event dead time and to write data to tape at a rate of 10 Mbytes/s. Data were written to tape continuously, including the periods between beam pulses (allowing all the collected data to be written to tape).

We have searched for the pentaquark decay $P^0_{\bar{c}s} \to K^{*0}K^-p$ in which the K^{*0} subsequently decays to $K^+\pi^-$. We normalize to the signal observed for $D_s^- \to K^{*0}K^-$ where the K^{*0} subsequently decays to $K^+\pi^-$. The $P^0_{\bar{c}s}$ and D_s^- decays share significant features so that several systematic errors common to both decay modes cancel in the ratio of cross section times branching fraction. We calculate the relative acceptance of our detector for these two modes using a Monte Carlo simulation. The production of the $P^0_{\bar{c}s}$ was modeled using the PYTHIA particle generator [17]. The pentaquarks were given a lifetime of 0.4 ps and masses of 2.75 and 2.83 GeV/c^2. Acceptances for other pentaquark lifetimes were obtained by weighting Monte Carlo generated events. Acceptances for other pentaquark masses were obtained by interpolating and extrapolating. Each $P^0_{\bar{c}s}$ was introduced into the LUND list of particles (replacing the $\overline{\Xi}^0_c$) and was forced to decay to $K^{*0}K^-p \to K^+K^-\pi^-p$. This method resulted primarily in centrally produced P^0's, with an x_F distribution of approximately $(1-|x_F|)^{4.4}$ for the x_F range where we have acceptance. This value is typical of charm production. Pentaquark decay was modeled assuming a uniform phase space density for the $K^{*0}K^-p$ particles.

Data reconstruction and additional event selection (filtering) were done using offline parallel processing systems [18]. Events with evidence of well-separated production (primary) and decay (secondary) vertices were retained for further analysis. Candidate $P^0_{\bar{c}s} \to K^{*0}K^-p$ decays were selected from events in which at least one four-prong decay vertex could be reconstructed using any combination of good tracks. At the same time, candidate $D_s^- \to K^{*0}K^-$ decays (for normalization) were selected from events in which at least one three-prong decay vertex could be reconstructed. For both decay modes, the two kaon candidates were required to have opposite charge, and the total charge was required to be either zero (for the $P^0_{\bar{c}s}$ candidates) or -1 (for the D_s^- candidates). The K^{*0} candidate was required to have an invariant mass within 50 MeV/c^2 of the nominal K^{*0} mass, and the K^{*0} daughter tracks were required to pass within 50 μm of each other.

To avoid bias in determining $P^0_{\bar{c}s}$ selection criteria, we masked the signal region in the data sample ($2.75 - 2.91$ GeV/c^2) until the final criteria were determined. Most selection criteria were chosen to maximize $S/\sqrt{B}$, where S was the signal from a Monte Carlo simulation and B was the background rate in the data sample outside the signal region. In addition, we used the D_s^- data in conjunction with Monte Carlo simulations to determine the optimal Čerenkov cuts for the kaons, and we used the $D^0 \to K^-\pi^-\pi^+\pi^+$ data in conjunction with Monte Carlo simulations to determine some of the vertex separation and other topological criteria.

The $P^0_{\bar{c}s}$ decay vertex was required to be well-separated from the production vertex with $\Delta z > 10\,\sigma_z$, where Δz is the separation between the two vertices and σ_z is the error on Δz. The decay vertex was required to lie outside the target foils and other solid material. We required $d > 2.5\,\sigma_d$, where d is the distance to the closest solid material and σ_d is the error on d. The decay vertex had to be isolated from its neighboring tracks by at least 10 μm. The momentum vector of the $P^0_{\bar{c}s}$ candidate was required to point back to the primary vertex with an impact parameter less than 30 μm. At least three of the four tracks had to belong to a secondary vertex candidate identified at the filter stage. In addition, we required the tracks in the vertex to point back to the secondary vertex more consistently than to the primary vertex – most importantly, we required that $\Pi_i(r_s/r_p) < 0.001$, where r_p is the impact parameter of a track with respect to the primary vertex, r_s is the impact parameter of a track with respect to the secondary vertex, and the product runs over all tracks i in the secondary vertex.

The Čerenkov detectors were used to identify charged π, K, and p candidates using an algorithm which compared the light collected in the cells of each detector with the level expected for each mass hypothesis for a track having the measured momentum[15]. Nominal probabilities for each hypothesis were calculated. Kaon candidates were required to have momenta greater than 6 GeV/c and to produce less light than expected for pions. This requirement produced efficiencies greater than 60% for real kaons with momenta between 6 and 36 GeV/c (and decreasing for greater momenta) and excluded approximately 85% of real pions and 60% of real protons. We also required that the product of the two kaon candidates' kaon Čerenkov probabilities be greater than a nominal value; this further reduced background by 40% while reducing signal efficiency by only 5%. Proton candidates were required to have momenta in the range $21 - 75$ GeV/c, where the Čerenkov detectors could discriminate most reliably between protons and kaons. The proton momentum range plus Čerenkov identification criteria yielded an efficiency for real protons greater than 45% while excluding 90% of real pions and 75% of real kaons.

We required that the sum of the squared transverse momenta ($\sum p_t^2$) of the four tracks, relative to the candidate $P^0_{\bar{c}s}$ direction, be greater than 0.5 (GeV/c)^2.

The Q-value of the $P^0_{\bar{c}s}$ decay (about 700 – 800 MeV/c^2 for binding energies in the range theoretically expected) determines the spectrum for this quantity, so the efficiency was determined directly using the Monte Carlo simulation. We checked that the Monte Carlo correctly produced the corresponding $\sum p_t^2$ spectra for decays of other particles.

We eliminated potential background by excluding events in which the K^{*0} candidate momentum vector projected back to the primary vertex with an impact parameter less than 40 μm; by excluding events in which the two kaon candidates formed a good $\phi \to K^+K^-$ candidate; and by excluding events in which either kaon or proton candidates pointed to a small region of the Čerenkov detector with a gap in the mirror planes at beam elevation. We also eliminated candidates in which one of the tracks was consistent with emerging from a secondary interaction in one of the target foils. Finally, we removed all $K^+K^-\pi^-p$ candidates which had invariant masses consistent with that of the D^0 when identified as $K\pi\pi\pi$.

The selection criteria for the candidate $D_s^- \to K^{*0}K^-$ decays used for normalization were as similar as possible to those used for the candidate $P^0_{\bar{c}s} \to K^{*0}K^-p$ decays, to minimize uncertainty in the relative acceptance. The kaon identification and kinematic criteria were identical. The topological criteria (vertex separation, isolation, etc.) were nominally the same but resulted in different efficiencies because three-prong decays and four-prong decays differ kinematically. The ratios of efficiencies as functions of $P^0_{\bar{c}s} \to K^{*0}K^-p$ lifetime and mass were studied using Monte Carlo simulations, and the results are discussed below.

Following the final determination of the selection criteria, we unmasked the signal region and observed the $K^+K^-\pi^-p$ invariant mass spectrum shown in Fig. 1. The events in the expected signal region, $2.75 - 2.91$ GeV/c^2, are cross-hatched. The expected resolution for a $P^0_{\bar{c}s} \to K^{*0}K^-p$ signal is approximately 11 MeV/c^2. One event above the D_s^-p threshold is kinematically consistent with the D_s^-p hypothesis and one is kinematically consistent with the D^-p hypothesis (with $D^- \to K^-K^+\pi^-$). These two events are denoted with slanted lines. No structure is evident in this spectrum, and we calculate upper limits on the ratio of cross section times branching fraction for the $P^0_{\bar{c}s}$ decaying into $K^{*0}K^-p$ relative to that for D_s^- decaying into $K^{*0}K^-$.

In Fig. 2 we show the invariant mass distribution of $K^+K^-\pi^-$ candidates which pass our $D_s^- \to K^{*0}K^-$ selection criteria. The background under the D_s^- signal is highly asymmetric; Cabibbo-favored $D^- \to K^+\pi^-\pi^-$ signal events that are misidentified as $K^+K^-\pi^-$ form a reflection which preferentially populates the region above the D_s^- mass. We fit the data in the D_s^- mass region using maximum likelihood fits with backgrounds based on the levels observed both below and above the signal region. From these fits we estimate a signal of 725 ± 88 $D_s^- \to K^{*0}K^-$ events. The error includes both statistical and systematic errors; it is dominated by the systematic uncertainty in the shape and level of the $D^- \to K^+\pi^-\pi^-$ reflection under the D_s^- signal.

We use the spectrum of Fig. 1 and the number of D_s^- events extracted from Fig. 2 to calculate 90% C.L. upper limits on the ratio of cross section times branching fraction for the $P^0_{\bar{c}s}$ decaying to $K^{*0}K^-p$ relative to that for D_s^- decaying to $K^{*0}K^-$. For a particular $K^{*0}K^-p$ invariant mass, we calculate the upper limit ξ as follows:

$$\xi\left(\frac{\sigma_P \cdot B_{P\to K^*Kp}}{\sigma_{D_s} \cdot B_{D_s\to K^*K}}\right) = \frac{\mu/\varepsilon_{P\to K^*Kp}}{N_{D_s\to K^*K}/\varepsilon_{D_s\to K^*K}}\,. \tag{1}$$

In this equation, μ is the 90% C.L. upper limit (see page 177 in ref. [9]) on the number of $P^0_{\bar{c}s} \to K^{*0}K^-p$ decays in a 40 MeV/c^2 mass range (the ranges specified in Table 1), given the number of events observed. This expression includes background as potential signal, and thus we arrive at a conservative upper limit. The quantity $N_{D_s\to K^*K}$ is the 725 ± 88 decays obtained from the normalization sample (Fig. 2). The quantities $\varepsilon_{P\to K^*Kp}$ and $\varepsilon_{D_s\to K^*K}$ are the detection efficiencies for $P^0_{\bar{c}s} \to K^{*0}K^-p$ and $D_s^- \to K^{*0}K^-$, respectively, obtained from the Monte Carlo simulation. The $P^0_{\bar{c}s} \to K^{*0}K^-p$ efficiency depends on the pentaquark mass and lifetime. For $M(P^0_{\bar{c}s}) = 2.83$ GeV/c^2 and $\tau(P^0_{\bar{c}s}) = 0.40$ ps, we find $\varepsilon_{P\to K^*Kp}/\varepsilon_{D_s\to K^*K} \approx 0.29$ (with $\varepsilon_{D_s\to K^*K} = 0.4\%$); the systematic error on this ratio is discussed below. We determine limits in the mass range extending from the lowest mass expected based on the color-hyperfine interaction (2.75 GeV/c^2) to the threshold for strong decay of the $P^0_{\bar{c}s}$ (2.91 GeV/c^2).

Systematic uncertainties arise from discrepancies between the data and the Monte Carlo simulations and from assumptions made about the pentaquark production mechanism. We estimate one-standard-deviation Gaussian errors for a variety of sources (the most important of which are discussed below), add the resulting fractional errors in quadrature, and then increase the upper limits obtained from Eq. 1 by a correction factor following the prescription of Cousins and Highland[19]. The upper limit on the number of observed candidates, μ, in Eq. (1) is replaced by

$$\mu' = \mu\left[1 + (\mu - \mathcal{S}) \times \frac{\mathcal{E}^2}{2}\right]\,. \tag{2}$$

Here, μ is the upper limit on the number of events as used in Eq. (1), $\mathcal{S}$ is the number of data events observed, and $\mathcal{E}$ is the sum in quadrature of the (fractional) statistical and systematic errors.

Varying the exponent of $(1-|x_F|)^n$ in the Monte Carlo simulation of the pentaquark by $\pm$ 1 changes the acceptance by 10%, and we use this value for the fractional uncertainty in acceptance due to our lack of knowledge of the production dynamics. A study of protons originating from $\Lambda \to \pi^- p$ decays found a 12% difference between Čerenkov efficiency in Monte Carlo simulation and in data, and we include this as an additional systematic uncertainty. Studies of our vertex selection algorithm give an uncertainty of 8% in the ratios of the efficiencies for the $P^0_{\bar{c}s}$ and the corresponding D^-_s decays. The statistical uncertainties in the Monte Carlo simulations lead to a 7% uncertainty in the ratio of the reconstruction efficiencies for the $P^0_{\bar{c}s}$ and the corresponding D^-_s decay. Most other selection criteria produced efficiencies which cancel in the ratio of cross section times branching fraction, and each of the other systematic uncertainties studied contributed a fractional error of less than 4%. The systematic uncertainties added in quadrature total 20%.

The upper limits we obtain for four mass bins are listed in Table 1. The first column specifies the mass range. The second column shows the ratio of Monte Carlo efficiencies for that range, assuming $\tau(P^0_{\bar{c}s}) = 0.40\,\mathrm{ps}$. The third column lists the number of events observed in that range. The fourth column lists the 90% C.L. upper limits on the number of $P^0_{\bar{c}s} \to K^{*0}K^- p$ decays (assuming no background), and the fifth column lists the effective upper limits on the number of decays calculated according to the prescription of Cousins and Highland (see Eq. 2). The last column gives the final upper limit on the ratio of cross section times branching fraction for $P^0_{\bar{c}s} \to K^{*0}K^- p$ relative to that for $D^-_s \to K^{*0}K^-$.

The $P^0_{\bar{c}s}$ detection efficiency is a strong function of lifetime, and theoretical estimates of the lifetime range over an order of magnitude. In Fig. 3(a) we show the acceptance for a 2.83 GeV/c^2 $P^0_{\bar{c}s}$ as a function of lifetime. At short lifetimes the decay vertices are not well-separated from the primary vertices. At long lifetimes many of the decay vertices extend beyond our fiducial volume. In the range 0.1 ps - 1.0 ps, where one expects the pentaquark lifetime to lie, the acceptance is increasing monotonically with lifetime. This leads to upper limits which decrease as lifetime increases, as shown in Fig. 3(b). For $P^0_{\bar{c}s}$ lifetimes one half that of the D^-_s or greater, our upper limits on the ratio of cross section times branching fraction are a few percent. To the extent that the branching fractions for $P^0_{\bar{c}s} \to K^{*0}K^- p$ and $D^-_s \to K^{*0}K^-$ are the same, the limits on cross section times branching fraction constrain the pentaquark production cross section to be less than a few percent of that for the D_s^-.

The results of this study are very similar to those of an earlier one in which we found 90% C.L. upper limits for the ratios of cross section times branching fraction for $P^0_{\bar{c}s} \to \phi\pi^- p$ relative to those for $D_s^- \to \phi\pi^-$[13]. For that ratio we obtained limits that were $2\% - 4\%$ for the $P^0_{\bar{c}s}$ mass range $2.75 - 2.91\mathrm{GeV}/c^2$. However, limits on ratios of production cross sections times branching fractions do not translate directly into limits on relative production cross sections for the parent particles. Although the branching fractions for $D_s^- \to K^{*0}K^-$ and for $D_s^- \to \phi\pi^-$ are very similar, and the ratio of corresponding branching fractions for $P^0_{\bar{c}s}$ would also be similar for a pentaquark that is dominantly an off-shell D_s^- and a spectator proton, other models of pentaquarks give different ratios of branching fractions. For example, another simple model assumes the matrix elements are the same for the three-body final states $K^{*0}K^-p$ and $\phi\pi^-p$ (as is true for the corresponding two-body matrix elements in D_s^- decay), and that they are constant over the Dalitz plot. The ratio of branching fractions is then determined by three-body phase space. In this case, $\Gamma(P^0_{\bar{c}s} \to \phi\pi^- p)/\Gamma(P^0_{\bar{c}s} \to K^{*0}K^- p) \approx 1.95$ for a $P^0_{\bar{c}s}$ mass of 2.75 GeV/c^2 and decreases linearly to a value ≈ 1.70 for a $P^0_{\bar{c}s}$ mass of 2.91 GeV/c^2. Thus the $\phi\pi^- p$ branching fraction would be larger than the $K^{*0}K^- p$ branching fraction, and the limits on $P^0_{\bar{c}s}$ cross section would be more stringent from the $\phi\pi^- p$ measurement.

In summary, we have searched for the decay of a bound pentaquark via its decay $P^0_{\bar{c}s} \to K^{*0}K^- p$. We chose our selection criteria while masking the signal region in the data sample to avoid bias. We see no evidence of this final state in our data. For pentaquarks having mass in the range 2.75 GeV/c^2 to 2.91 GeV/c^2 and lifetimes of 0.4 ps, we obtain upper limits that lie in the range $1.6\% - 3.6\%$ for the ratio of $\sigma \cdot B$ for $P^0_{\bar{c}s} \to K^{*0}K^- p$ relative to that for $D_s^- \to K^{*0}K$. Depending on assumptions made about decay mechanisms, the limits on the ratios of cross section times branching fraction can be converted into limits on ratios of production cross sections. These upper limits approach the theoretical predictions.

We thank Dr. Harry Lipkin for many fruitful discussions. We gratefully acknowledge the staffs of Fermilab and of all the participating institutions. This research was supported by the Brazilian Conselho Nacional de Desenvolvimento Científico e Technológio, the Mexican Consejo Nacional de Ciencia y Tecnologica, the Israeli Academy of Sciences and Humanities, the United States Department of Energy, the U.S.-Israel Binational Science Foundation, and the United States National Science Foundation. Fermilab is operated by the Universities Research Association, Inc., under contract with the United

States Department of Energy.

References

[1] R.L. Jaffe, Phys. Rev. Lett. **38** (1977) 195.

[2] J. Belz *et al.*, Phys. Rev. Lett. **76** (1996) 3277, Phys. Rev. **C56** (1997) 1164, Phys. Rev. **D53** (1996) R3487;
R.W. Stotzer *et al.*, Phys. Rev. Lett. **78** (1997) 3646, and references therein.

[3] H.J. Lipkin, *Proc. of the XXII$^{\underline{nd}}$ Rencontre de Moriond*, France, J. Tran Thanh Van *ed.*, Editions Frontieres, Gif-sur-Yvette, France (1987) 691; H.J. Lipkin, Phys. Lett. **B195** (1987) 484.

[4] C. Gignoux *et al.*, Phys. Lett. **B193** (1987) 323.

[5] S. Takeuchi, S. Nussinov, and K. Kubodera, Phys. Lett. **B318** (1993) 1.

[6] S. Zouzou and J.M. Richard, *Few-Body Systems* **16** (1994) 1.

[7] S. Fleck *et al.*, Phys. Lett. **B220** (1989) 616.

[8] D.O. Riska and N.N. Scoccola, Phys. Lett. **B299** (1993) 338;
Y. Oh, B.Y. Park, and D.P Min, Phys. Rev. **D50** (1994) 3350;
Y. Oh, B.Y. Park, and D.P Min, Phys. Lett. **B331** (1994) 362;
C.K. Chow, Phys. Rev. **D51** (1995) 6327;
C.K. Chow, Phys. Rev. **D53** (1996) 5108.

[9] Review of Particle Properties, C. Caso *et al.*, European Physical Journal **C3** (1998).

[10] H.J. Lipkin, Nuclear Physics **B21** (1991) 258.

[11] S. MayTal-Beck *et al.*, *Proc. of the 8$^{\underline{th}}$ Meeting, Div. of Particles and Fields of the Am. Phys. Soc.*, S. Seidel *ed.*, World Scientific, Singapore (1994) 1177, and references therein.

[12] M. A. Moinester, D. Ashery, L. G. Landsberg, and H. J. Lipkin, Z. Phys. **A356** (1996) 207.

[13] E.M. Aitala *et al.*, Phys. Rev. Lett. **81** (1998) 44.

[14] J. A. Appel, Ann. Rev. Nucl. Part. Sci. **42** (1992) 367, and references therein;
D. J. Summers *et al.*, *Proc. of the XXVII$^{\underline{th}}$ Rencontre de Moriond*, France, J. Tran Thanh Van *ed.* , Editions Frontieres (1992), 417;
E. M. Aitala *et al.*, Phys. Rev. Lett. **76** (1996) 364.

[15] D. Bartlett *et al.*, Nucl. Instr. and Meth. **A260** (1987) 55.

[16] S. Amato *et al.*, Nucl. Inst. and Meth. **A324** (1993) 535.

[17] T. Sjöstrand, Computer Physics Commun. **82** (1994) 74.

[18] F. Rinaldo and S. Wolbers, Computers in Physics **7** (1993) 184;
S. Bracker *et al.*, IEEE Trans. Nucl. Sci. **43** (1996) 2457.

[19] R.D. Cousins and V.L. Highland, Nucl. Instr. and Meth. **A320** (1992) 331.

Table 1
Upper limits on the ratio of cross section times branching fraction for $P^0_{\bar{c}s} \to K^{*0}K^-p$ relative to that for $D_s^- \to K^{*0}K^-$, in four mass ranges. The 90% C.L. upper limits on the total numbers of events observed in the bins (μ) are increased to account for systematic uncertainties following the prescription of Cousins and Highland. We use these corrected values (μ') to calculate the upper limits listed in the last column.

Mass [GeV/c^2]	$\varepsilon_{P\to K^*Kp}/\varepsilon_{D_s\to K^*K}$	Events	μ	μ'	Upper Limit
2.75-2.79	0.23	3	5.77	6.1	0.036
2.79-2.83	0.27	1	3.30	3.5	0.018
2.83-2.87	0.31	1	3.30	3.5	0.016
2.87-2.91	0.35	2	4.49	4.7	0.019

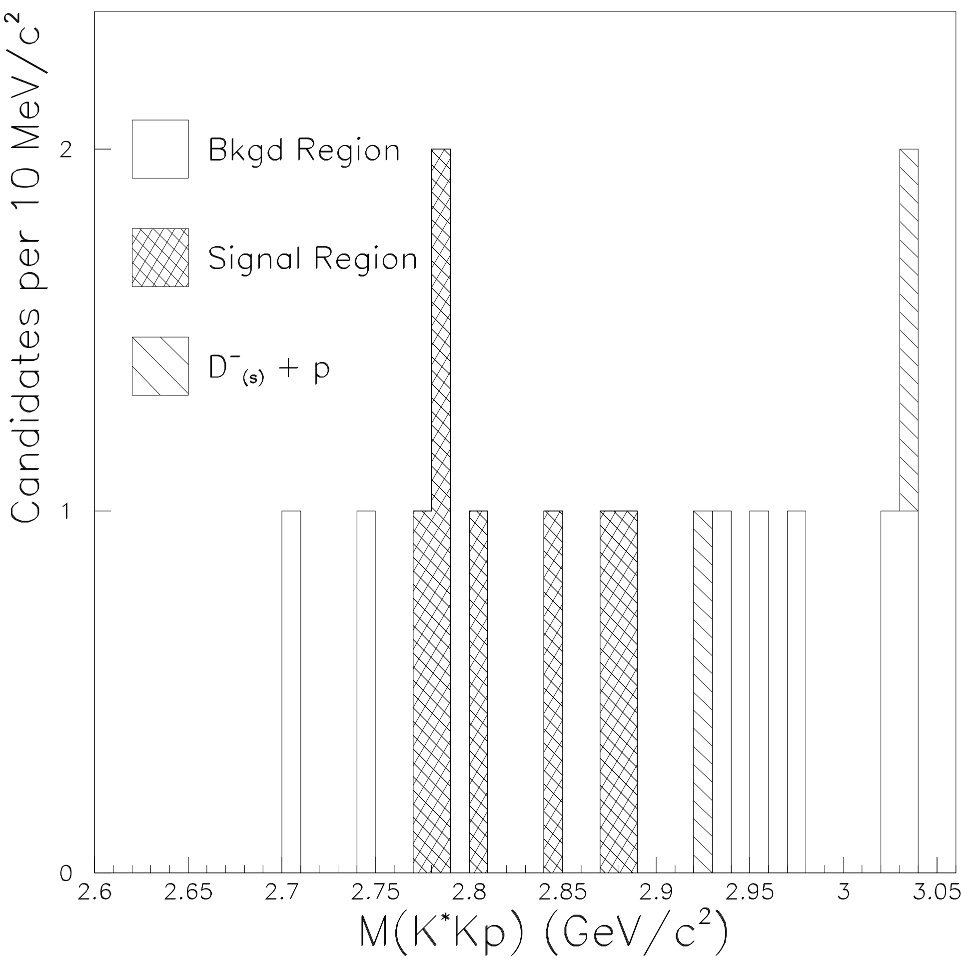

Fig. 1. The $K^-K^+\pi^-p$ invariant mass distribution for the events which satisfy the final $P^0_{\bar{c}s} \to K^{*0}K^-p$ selection criteria described in the text. To avoid bias, the signal region from 2.75 GeV/c^2 to 2.91 GeV/c^2 (in which the events have been cross-hatched) was masked until the selection criteria were determined. The events denoted with slanted lines are kinematically consistent with either the D_s^-p hypothesis or the D^-p hypothesis.

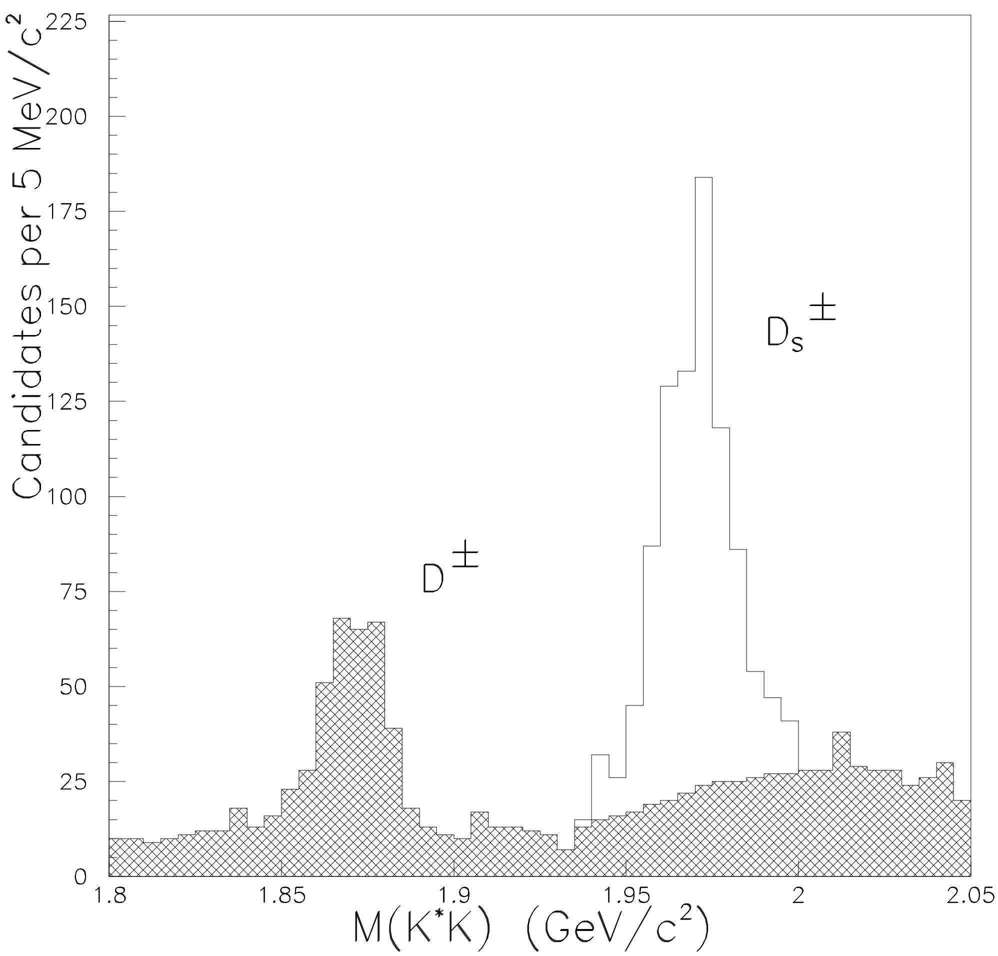

Fig. 2. The $K^-K^+\pi^-$ invariant mass distribution for events which satisfy the final $K^{*0}K^-$ selection criteria described in the text. The D_s^- normalization signal is seen clearly. The level of the background under the D_s^- signal was determined from the background levels observed above and below the signal region and from studies of $D^- \to K^+\pi^-\pi^-$ reflections, as discussed in the text. The part of the shaded area in the D_s signal region indicates the overall level of the background there.

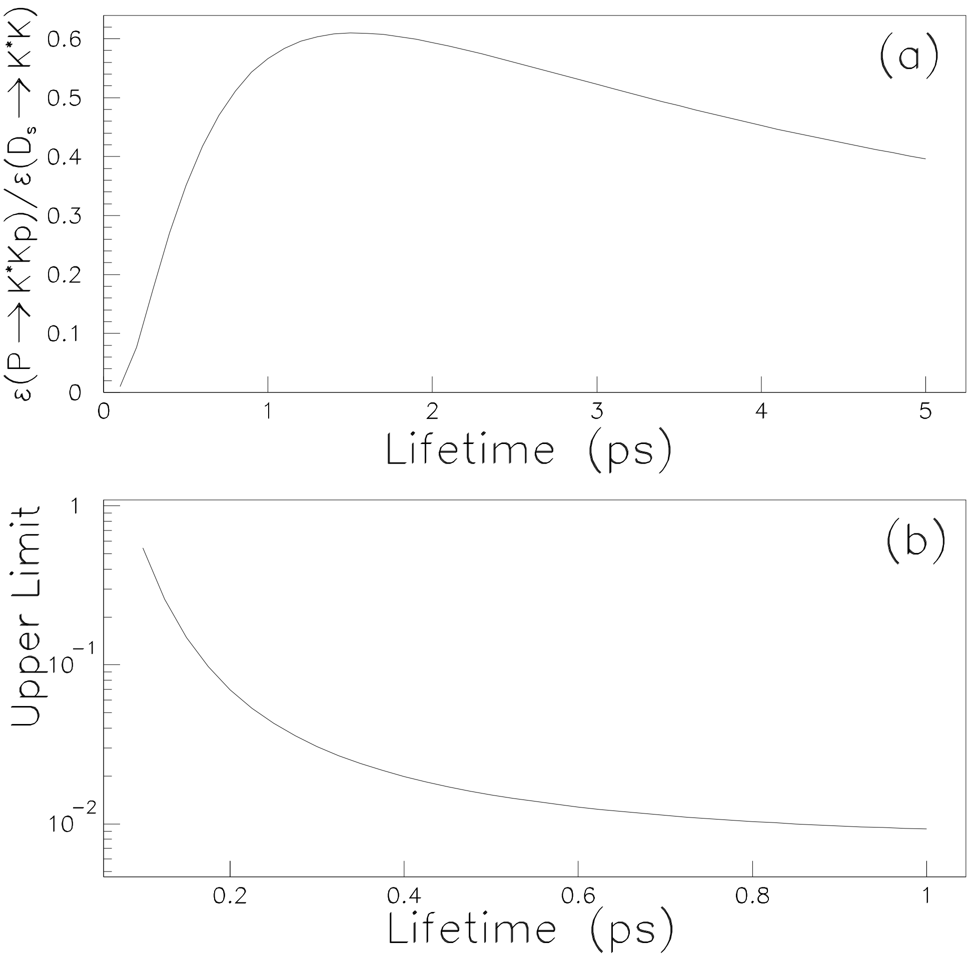

Fig. 3. (a) The ratio $\varepsilon_{P\to K^*Kp}/\varepsilon_{D_s\to K^*K}$ for a $P^0_{\bar{c}s}$ of mass 2.83 GeV/c^2, as a function of $P^0_{\bar{c}s}$ lifetime. (b) The upper limit on the ratio of cross section times branching fraction for $P^0_{\bar{c}s} \to K^{*0}K^-p$ relative to that for $D_s^- \to K^{*0}K^-$, as a function of $P^0_{\bar{c}s}$ lifetime.